AGU PUBLICATIONS

JGR

Journal of Geophysical Research: Atmospheres

RESEARCH ARTICLE

10.1002/2015JD023953

Key Points:
- We examine the sensitivity of AA to background SIC
- A clear nonlinear relationship between the Arctic warming trend and mean SIC
- Sea ice albedo and turbulent heat flux feedbacks play a key role in the nonlinear relationship

Correspondence to:
J.-S. Kug,
jskug@postech.ac.kr

Citation:
Yim, B. Y., H. S. Min, B.-M. Kim, J.-H. Jeong, and J.-S. Kug (2016), Sensitivity of Arctic warming to sea ice concentration, *J. Geophys. Res. Atmos.*, *121*, 6927–6942, doi:10.1002/2015JD023953.

Received 20 JUL 2015
Accepted 3 JUN 2016
Accepted article online 11 JUN 2016
Published online 27 JUN 2016

Sensitivity of Arctic warming to sea ice concentration

Bo Young Yim[1], Hong Sik Min[2], Baek-Min Kim[3], Jee-Hoon Jeong[4], and Jong-Seong Kug[5]

[1]Climate Prediction Division, Korea Meteorological Administration, Seoul, South Korea, [2]Korea Institute of Ocean Science and Technology, Ansan, South Korea, [3]Korea Polar Research Institute, Incheon, South Korea, [4]Department of Oceanography, Chonnam National University, Gwangju, South Korea, [5]School of Environmental Science and Engineering, Pohang University of Science and Technology (POSTECH), Pohang, South Korea

Abstract We examine the sensitivity of Arctic amplification (AA) to background sea ice concentration (SIC) under greenhouse warming by analyzing the data sets of the historical and Representative Concentration Pathway 8.5 runs of the Coupled Model Intercomparison Project Phase 5. To determine whether the sensitivity of AA for a given radiative forcing depends on background SIC state, we examine the relationship between the AA trend and mean SIC on moving 30 year windows from 1960 to 2100. It is found that the annual mean AA trend varies depending on the mean SIC condition. In particular, some models show a highly variable AA trend in relation to the mean SIC clearly. In these models, the AA trend tends to increase until the mean SIC reaches a critical level (i.e., 20–30%), and the maximum AA trend is almost 3 to 5 times larger than the trend in the early stage of global warming (i.e., 50–60%, 60–70%). However, the AA trend tends to decrease after that. Further analysis shows that the sensitivity of AA trend to mean SIC condition is closely related to the feedback processes associated with summer surface albedo and winter turbulent heat flux in the Arctic Ocean.

1. Introduction

In the recent decades, the surface warming over the Arctic has been almost twice as large as the warming over the rest of the globe, the so-called "Arctic amplification (AA)" [*Graversen et al.*, 2008; *Serreze et al.*, 2009; *Screen and Simmonds*, 2010; *Screen et al.*, 2012]. There have been many studies discussing impacts of AA not only on local changes surrounding the Arctic Ocean [*Symon et al.*, 2004; *Stroeve et al.*, 2007] but also on large-scale climate system in the midlatitudes [*Francis et al.*, 2009; *Honda et al.*, 2009; *Deser et al.*, 2010; *Overland and Wang*, 2010; *Overland et al.*, 2011; *Screen and Simmonds*, 2013; *Screen et al.*, 2014; *Simmonds and Govekar*, 2014; *Kug et al.*, 2015; *Perlwitz et al.*, 2015; *Yim et al.*, 2016]. Although it is still a controversial issue whether AA can modulate weather and climate in the midlatitudes, the rapidly changing Arctic has drawn much attention in terms of both local and global climate changes.

Many studies have tried to understand the underlying physical mechanisms that are responsible for the AA, including local feedback associated with the decline of sea ice extent [*Serreze et al.*, 2009; *Overland and Wang*, 2010; *Screen and Simmonds*, 2010], atmospheric and oceanic transports [*Graversen et al.*, 2008; *Kug et al.*, 2010; *Screen et al.*, 2011; *Alexeev and Jackson*, 2013; *Koenigk and Brodeau*, 2014; *Rudeva and Simmonds*, 2015], and feedbacks associated with changes in temperature, clouds, water vapor, snow cover, and vegetation [*Liu et al.*, 2008; *Graversen and Wang*, 2009; *Derksen and Brown*, 2012; *Jeong et al.*, 2012, 2014; *Pithan and Mauritsen*, 2014]. Among them, the Arctic sea ice is known to be a primary physical contributor to the AA, because it controls incoming solar radiation in association with the surface albedo feedback and the heat exchange between the cold atmosphere and the warmer, ice-covered ocean. *Screen and Simmonds* [2010] suggested that summer Arctic sea ice that has experienced remarkable reduction in recent years plays a critical role in the AA, which is the strongest at the surface in the following cold seasons. Observational and modeling studies consistently showed that reduction in sea ice leads to increased incoming solar heating into the open ocean by decreasing the surface albedo [*Holland and Bitz*, 2003; *Zhang and Walsh*, 2006; *Perovich et al.*, 2007]. This reduction in sea ice has also been related to changes in ocean-atmosphere heat fluxes, with its characteristics insulating the ocean from the overlying cold atmosphere. Increased absorption of incoming solar radiation at less ice-covered ocean surface is used to warm the upper ocean and melt ice around, and the heat stored in the ocean during summer leads to a greater release of heat to the atmosphere during the following autumn and winter [*Serreze and Francis*, 2006; *Francis et al.*, 2009; *Serreze et al.*, 2009; *Deser et al.*, 2010; *Screen and Simmonds*, 2010].

It is worth noting that the AA has been particularly strong in the recent decades, as mentioned above [*Polyakov et al*., 2002; *Serreze and Francis*, 2006; *Graversen et al*., 2008; *Serreze et al*., 2009; *Screen and Simmonds*, 2010; *Screen et al*., 2012], with the low September sea ice cover in the satellite record, especially after 2000 [*Comiso et al*., 2008; *Stroeve et al*., 2012, 2014; *Devasthale et al*., 2013; *Parkinson and Comiso*, 2013]. There are many studies concerning whether the greatly accelerated AA in the recent decades is caused by internal variability or external forcing [*Holland and Bitz*, 2003; *Stroeve et al*., 2007, 2012; *Holland et al*., 2008; *Serreze et al*., 2009; *Kattsov et al*., 2010; *Screen and Simmonds*, 2010; *Kay et al*., 2011]. For example, *Serreze et al*. [2009] and *Screen and Simmonds* [2010] suggested that the rapid reduction in sea ice plays a leading role in accelerating the AA. *Kay et al*. [2011] described highly variable Arctic sea ice trends in the late twentieth century using the Community Climate System Model version 4 (CCSM4) simulations and showed that both internal variability and external anthropogenic forcing influence the magnitude of Arctic sea ice trends from 1979 to 2005. However, it is still under debate as to what are the main causes of these rapid changes in AA.

Another critical issue is whether the recent large AA trend in the observations will continue or change in the future. In order to project the future AA, it is quite important to understand what can determine the speed of the Arctic warming for a given external radiative forcing. Recent studies using the model output from the Coupled Model Intercomparison Project Phase 5 (CMIP5) simulations reported that the Arctic sea ice extent properties and the recent sea ice decline are better reproduced in the CMIP5 models than in the Coupled Model Intercomparison Project Phase 3 (CMIP3) models, although some other biases still remain in the CMIP5 models [*Maslowski et al*., 2012; *Stroeve et al*., 2012, 2014; *Wang and Overland*, 2012; *Xu et al*., 2013; *Simmonds*, 2015]. Furthermore, there has been an attempt to understand the relation between surface air temperature and sea ice using the CMIP3 models and observations. *Mahlstein and Knutti* [2012] showed that the total sea ice area is approximately linearly related to Arctic surface air temperature and suggested that September Arctic sea ice is predicted to disappear when there is about 2°C change in annual mean global surface temperature above present.

Many modeling studies focused on evaluating the performance of simulated Arctic sea ice and predicting when the Arctic will become nearly ice-free [*Wang and Overland*, 2009, 2012; *Massonnet et al*., 2012]. However, less attention has been paid to how the AA will change in the future and how it responds to varying sea ice states in the present day and future. In this study, we investigate how the surface-based AA trend is related to the mean sea ice properties, such as sea ice concentration (SIC). SIC represents sea ice area fraction, i.e., the portion of the area covered by sea ice over each of the grid square, ranging from 0% to 100%. Arctic [70°–90°N] and global near-surface air temperature trends are calculated, and their difference is defined as the AA trend in the present study, to roughly exclude model's global sensitivity to external forcing (e.g., CO_2). The purposes of this paper are to show how the AA trend changes depending on the mean Arctic SIC and to understand projections of the future AA trend in the CMIP5 models. We also attempt to understand the feedback processes involved in the relationship between the AA trend and mean SIC condition. Because the uncertainty in the Arctic temperature trend and sea ice properties of the CMIP5 models are reduced compared to that of the CMIP3 models to some extent [*Stroeve et al*., 2012; *Xu et al*., 2013], it is useful to investigate these relationships using the CMIP5 models.

The paper is organized as follows. Section 2 describes the CMIP5 multimodel data set and methods used in this study. In section 3, we evaluate and compare the present-day sea ice properties simulated by 23 coupled general circulation models (CGCMs). Based on the CMIP5 models, the relationship between the AA trend and mean Arctic SIC is presented, and detailed analysis of associated feedback processes is discussed. Summary and discussion are provided in section 4.

2. Models and Data Sets

The CGCMs used in this study are part of the World Climate Research Programme's CMIP5 multimodel data set and were performed for the Intergovernmental Panel on Climate Change's Fifth Assessment Report (AR5). The 23 CGCMs used are listed in Table 1. These models and their ensemble members are selected based on the availability of the outputs at the time of our analysis. Detailed information on the CMIP5 models and experiments is available at http://cmip-pcmdi.llnl.gov/cmip5/experiment_design.html [e.g., *Taylor et al*., 2012]. For the models that have several ensemble members, ensemble mean of each model was taken before multimodel ensemble mean (MME) is calculated. Thus, the MME is not biased toward models with more members.

Table 1. The CGCMs Used in This Study

Model	Number of Ensemble Members
1. CanESM2	5
2. CCSM4	6
3. CESM1-CAM5	3
4. CMCC-CM	1
5. CMCC-CMS	1
6. CSIRO-Mk3-6-0	1
7. FGOAL-g2	1
8. GISS-E2-H	2
9. GISS-E2-R	2
10. HadGEM2-AO	1
11. HadGEM2-CC	1
12. HadGEM2-ES	3
13. inmcm4	1
14. IPSL-CM5A-MR	1
15. IPSL-CM5B-LR	1
16. MIROC5	3
17. MIROC-ESM	1
18. MIROC-ESM-CHEM	1
19. MPI-ESM-LR	3
20. MPI-ESM-MR	1
21. MRI-CGCM3	1
22. NorESM1-M	1
23. NorESM1-ME	1

Two sets of the simulation data are used in the present study. The historical run from 1960 to 2005 is used here, which was run using changing conditions consistent with the observations that include atmospheric composition (including CO_2) due to both anthropogenic and volcanic influences, solar forcing, emissions or concentrations of short-lived species and natural and anthropogenic aerosols or their precursors, and land use. The other is the representative concentration pathway 8.5 (RCP8.5) scenario run from 2006 to 2100 for future climate change, in which the radiative forcing increases nearly steadily over the 21st century to peak at +8.5 W m^{-2} in 2100 relative to the preindustrial levels. Under the RCP8.5, almost all CGCMs reach the nearly sea ice-free condition in summer within the 21st century [*Massonnet et al*., 2012; *Wang and Overland*, 2012].

To assess the models' fidelity in reproducing the sea ice climatology in the present-day Arctic, we used the Hadley Centre Sea Ice and Sea Surface Temperature (HadISST) data set [*Rayner et al*., 2003] for the SIC from 1960 to 2012. Many studies have discussed the summer (or September) Arctic sea ice, which shows the minimum of annual SIC and undergoes a dramatic decrease in the recent decades [e.g., *Comiso et al*., 2008; *Stroeve et al*., 2008; *Wang and Overland*, 2009, 2012; *Massonnet et al*., 2012], typically to examine sea ice trend and its role because it can be considered as a good indicator of the thermodynamic state of the ice cover. Thus, we focus on the SIC in late summer and early fall from August to October (ASO), when it is the lowest. The SIC over the Arctic during 1960–2012 has the minimum in ASO in both the MME of the 23 analyzed CGCMs and the HadISST data set (not shown). The Arctic SIC in this study represents the SIC averaged over all ocean grids north of 70°N. Hereafter, SIC is referred to as the SIC averaged over the ASO season, if no other specification is given.

The sea ice state in this season can be related to Arctic temperature not only in the corresponding season but also in other following seasons in association with seasonally varying and interconnecting feedbacks, as pointed by *Deser et al*. [2010] and *Screen and Simmonds* [2010]. Thus, we examine the annual mean temperature trend in order to focus on long-term signals responding to the SIC. The annual mean near-surface (2 m) air temperature is averaged from August to July of the following year to examine its relation with the SIC. The overall results are not sensitive, although the starting month for the annual mean is changed. The temperature trend is computed using the linear least squares fitting.

To examine how the sensitivity of the Arctic warming for a given radiative forcing depends on the mean SIC, we calculate AA trend and mean SIC on moving 30 year windows from 1960 to 2100. Although other time windows, such as 20 year and 40 year, were also tested, the overall results are similar (not shown). Before the analysis, all oceanic and atmospheric outputs of the models and the observation data were regridded to the resolution of 1° × 1° and 2.5° × 2.5°, respectively.

3. Results

3.1. Evaluation of CMIP5 Models' Performance by Climatological Mean SIC

Prior to examining the relationship between the AA trend and mean SIC in these climate models, we first evaluate the CMIP5 models' performance of reproducing the climatological mean SIC in the present-day Arctic. The simulated Arctic SIC is compared among the CMIP5 models, together with the results of the observation and CMIP3 models presented by previous studies [*Stroeve et al*., 2007, 2012; *Massonnet et al*., 2012].

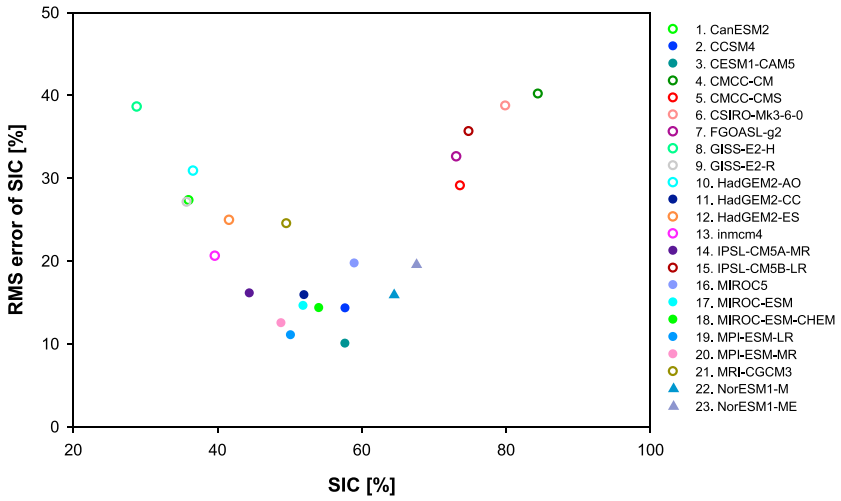

Figure 1. Scatter plot of climatological mean [1960–2012] Arctic [70°–90°N] ASO SIC and its RMS error in the 23 CGCMs. The models in which the simulated Arctic ASO SIC falls within ~20% range of that in the observation (56.2%), as in *Wang and Overland* [2012], and the RMS error of SIC that is smaller than the MME (23.2%) are marked by filled symbols.

Figure 1 shows the climatological mean SIC averaged over the Arctic Ocean [70°–90°N] and its root-mean-square (RMS) error for the reference period of 1960–2012 simulated by the 23 CGCMs. The RMS error is considered to reflect the reproducibility of the local distribution of SIC and is calculated by averaging the differences in the climatological mean SIC between each model and the observation for the same period over the Arctic [70°–90°N]. The climatological mean Arctic SIC in the MME (~54.9%) is in good agreement with that in the observation (~56.2%), which is closer to the observation than that of the CMIP3 models [*Stroeve et al*., 2007, 2012]. It ranges from 28.9% in the GISS-E2-H model to 84.5% in the CMCC-CM model. About half of the 23 models fall in the range of 20% with respect to the observation.

The RMS errors also reveal a considerable diversity among the CMIP5 models, with the MME of the RMS error (23.2%). As expected from the calculation of RMS error, the RMS errors tend to be smaller for the models with a reasonable performance of climatological mean SIC (except for MRI-CGCM3) (Figure 1). This indicates that on the whole the models with a reasonable Arctic-averaged SIC simulate the local sea ice distribution reasonably as well. In 11 out of the 23 CMIP5 (i.e., CCSM4, CESM1-CAM5, HadGEM2-CC, IPSL-CM5A-MR, MIROC5, MIROC-ESM, MIROC-ESM-CHEM, MPI-ESM-LR, MPI-ESM-MR, NorESM1-M, and NorESM1-ME), the simulated Arctic SIC falls within ~20% range of that in the observation, as in *Wang and Overland* [2012], and RMS error of SIC is smaller than the MME. These models include five out of the seven models suggested by *Wang and Overland* [2012] and five out of the nine models suggested by *Liu et al*. [2013]. Large intermodel differences in simulating sea ice properties are possibly associated with various specific features of individual CGCMs, such as circulation, transport, cloud, and radiation processes in the Arctic [e.g., *Eisenman et al*., 2007; *Holland et al*., 2010; *Kwok*, 2011]. These may lead to significant differences in projecting the Arctic climate in the models.

3.2. Relationship Between the AA Trend and Mean SIC

Based on the 23 CMIP5 models, we examine the relationship between the model's sensitivity of the Arctic warming and sea ice mean state for a given external forcing. We hypothesize that the sensitivity of the Arctic warming for a given radiative forcing depends on the mean SIC.

In order to examine the relationship between the AA trend and SIC mean state, the annual mean AA trends for mean Arctic SIC calculated on moving 30 year windows from 1960 to 2100 are shown in Figure 2. The projections show that the Arctic sea ice would reduce to a nearly ice-free state until 2100 in most models. It is shown that all models except for MRI-CGCM3 have positive AA trends under any mean SIC conditions. However, it is interesting that the AA trends vary with the mean SIC conditions in these models. Moreover, it is shown that in the early stage of global warming (i.e., large mean SIC), the AA trends increase largely with decreasing mean SIC in many models, indicating an accelerated AA as the SIC becomes smaller.

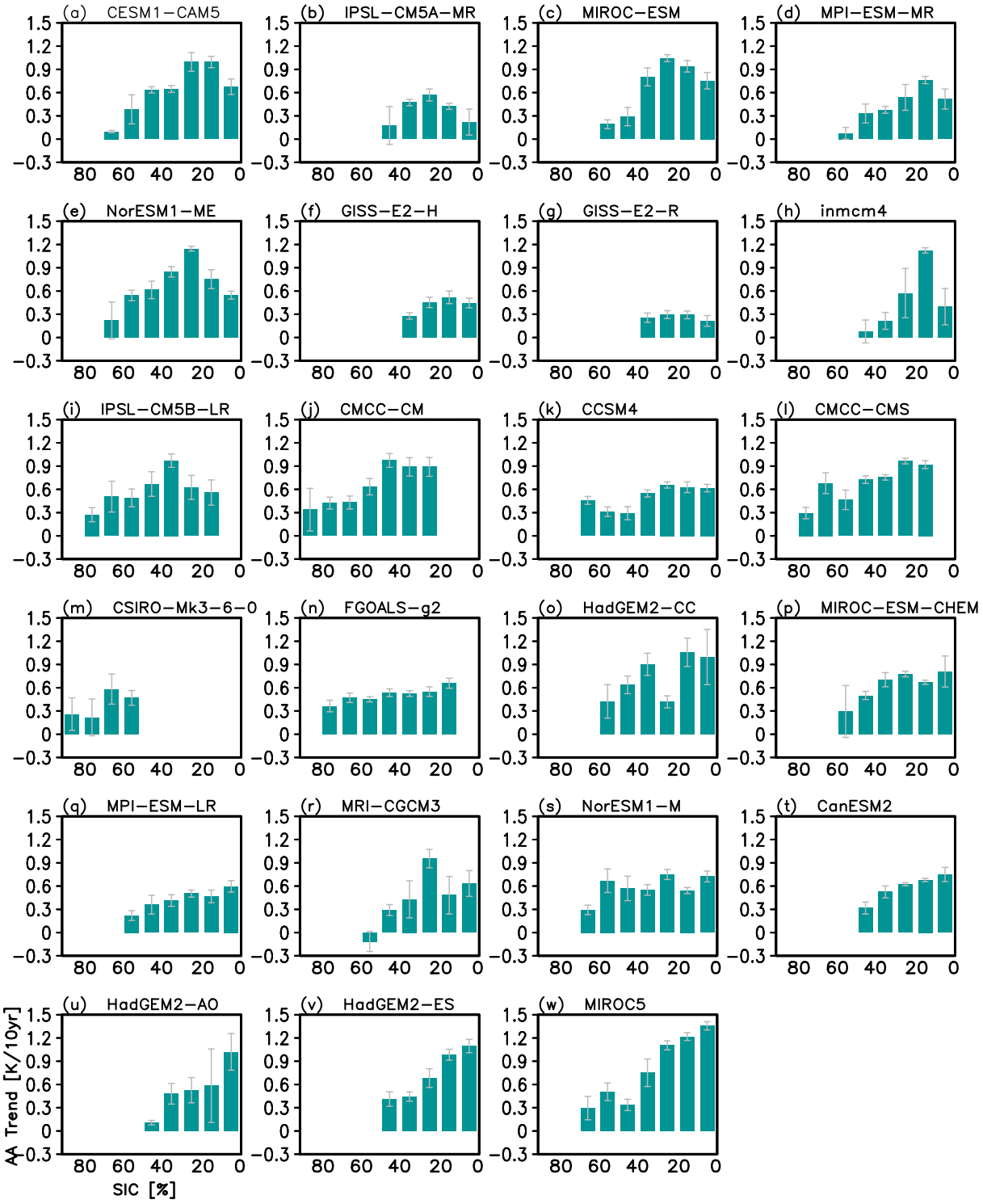

Figure 2. Histograms of annual mean AA trends for mean Arctic ASO SIC from the 23 models. The AA trends and mean Arctic SIC are calculated on moving 30 year windows. The error bars represent 1 standard deviation of the AA trends for each SIC range.

However, the sensitivity of the AA trend to mean SIC shows a somewhat different evolution among the CGCMs as greenhouse warming progresses further and the mean SIC becomes smaller. It is notable that some models project a highly variable AA trend depending on the mean SIC (Figures 2a–2j). In these models, the AA trend tends to increase until the mean Arctic SIC reaches a critical level (10–20% in the GISS-E2-H, inmcm4 and MPI-ESM-MR,

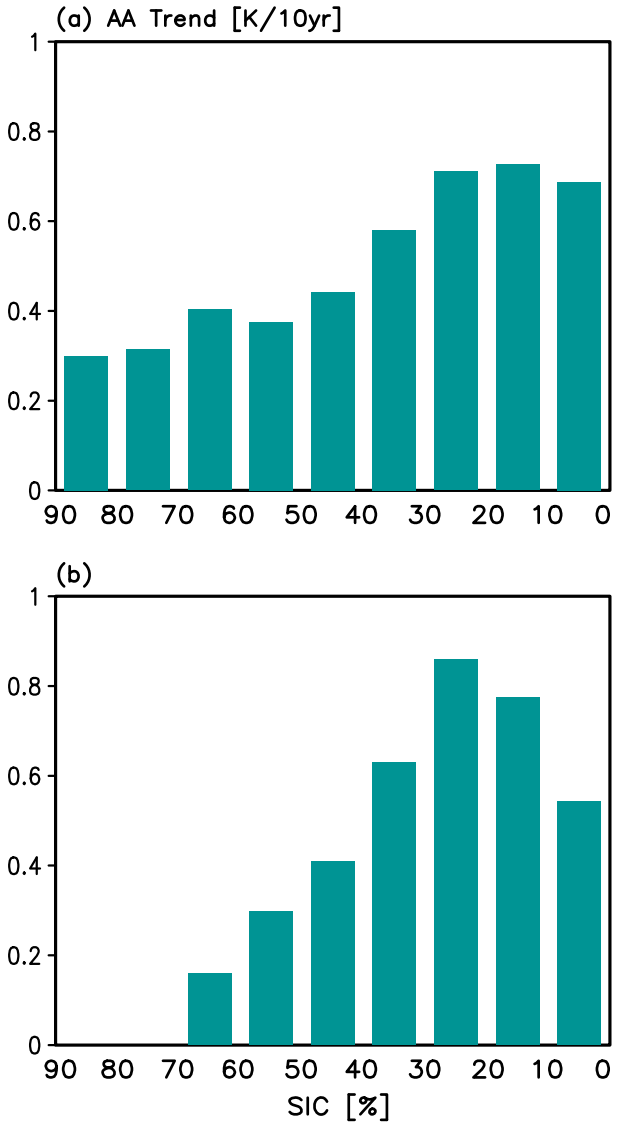

Figure 3. Same as Figure 2, except for the MME from the (a) 23 models and (b) five selected models.

20–30% in the CESM1-CAM5, GISS-E2-R, IPSL-CM5A-MR, MIROC-ESM, and NorESM1-ME, 30–40% in the IPSL-CM5B-LR, and 40–50% in the CMCC-CM), whereas the magnitude of the trend tends to rather decrease after that. The decrease in the AA trend for smaller mean SIC does not indicate that the Arctic becomes cooler. This indicates that the increasing rate of the Arctic warming is not as large as that in the past. These results imply that the responses of AA trends are nonlinear in relation to the mean Arctic SIC state in these models.

On the other hand, these relationships are not clear in some models, even though the AA trends show partly nonlinear behavior (Figures 2k–2s). Several models show continuously increasing AA trend with decreasing mean SIC (Figures 2t–2w).

Meanwhile, about half (Figures 2a–2e) of the 11 models simulating the present-day observed SIC state reasonably in Figure 1 show the clear relationship between the AA trend and mean SIC. These models are also half of the models representing the nonlinear responses of AA trend (Figures 2a–2j). This indicates that although the models simulate the present-day sea ice states reasonably, the projection of future changes can be different among the models.

Although the changes in the AA trends in Figure 2 show large diversity among the models, overall feature of the relationship between the AA trend and mean Arctic SIC in their MME (Figure 3a) resembles that in the models that show nonlinear responses (Figures 2a–2j). Figure 3a shows that as the mean Arctic SIC becomes smaller, the AA trend tends to increase; however, after it reaches a critical level (10–20%), it decreases. This indicates that the AA will still occur in a nearly sea ice-free state, but its changing rate will not continue to increase.

In order to illustrate the nonlinear responses of AA trends in detail, we select the models showing the nonlinear relationship between the AA trend and mean SIC clearly. Out of them, the models representing the mean SIC condition very dissimilar to the present-day observed SIC are excluded, and the five models, that is, CESM1-CAM5, IPSL-CM5A-MR, MIROC-ESM, MIROC-ESM-MR, and NorESM1-ME (Figures 2a–2e), are eventually selected. Considering the MME only from these five selected models, the AA trend shows larger changes with the mean SIC (Figure 3b). The AA trend for the mean SIC of 20–30% (0.86 K 10 yr^{-1}) is 5 times more than that of 60–70% (0.16 K 10 yr^{-1}) and almost 3 times larger than that of 50–60% (0.30 K 10 yr^{-1}). On the other hand, when the sea ice melts further and almost completely disappears (0–10%), the AA trend (0.54 K 10 yr^{-1}) is about 60% of the maximum trend.

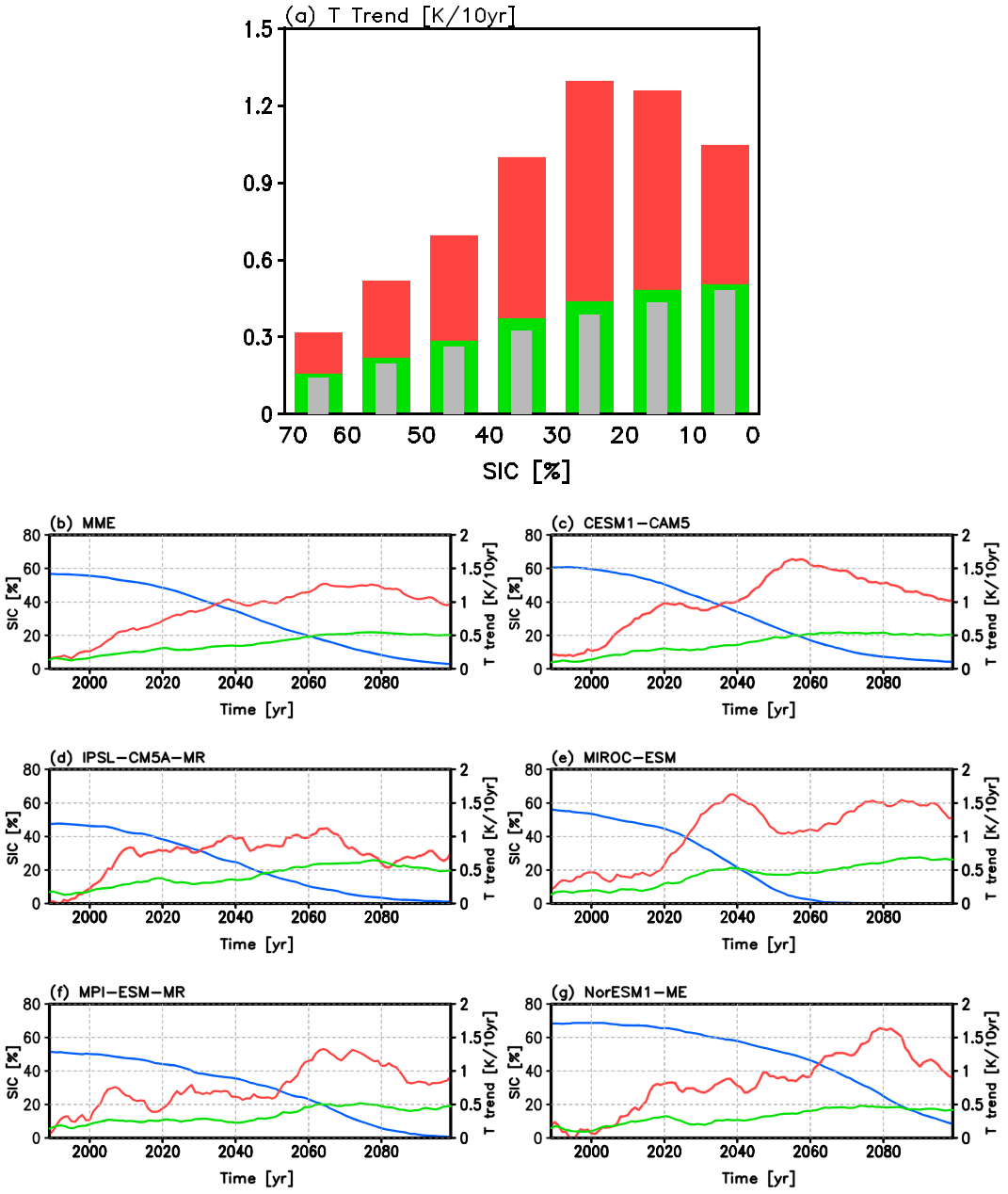

Figure 4. (a) Histograms of annual mean Arctic (red) and global (green) near-surface air temperature trends for mean Arctic ASO SIC in the MME of the five selected models and (b–g) time series of mean Arctic ASO SIC (blue) and annual mean Arctic (red) and global (green) near-surface temperature trends during 1960–2100 in the MME of the five selected models and each model. Gray bars in Figure 4a represent values for the temperature trends outside of the polar regions [50°S–50°N]. Values in Figures 4b–4g are marked in the corresponding year at the end of the 30 year windows [1989–2100].

Of course, it is not possible to know at the present stage which models will be closer to future changes. Nonetheless, detailed understanding of the nonlinear relationship between the AA trend and SIC mean state in these five selected models may provide important implications on prediction of the future Arctic climate changes. These models may reveal some unique features, such as feedback process between Arctic temperature and sea ice, and thus why the Arctic warming may not continue to amplify. Therefore, it is useful to examine the results of the five selected models that show the variable AA trend depending to the SIC mean state clearly, as depicted in Figures 2a–2e. Hereafter, we will focus on these models for further analysis.

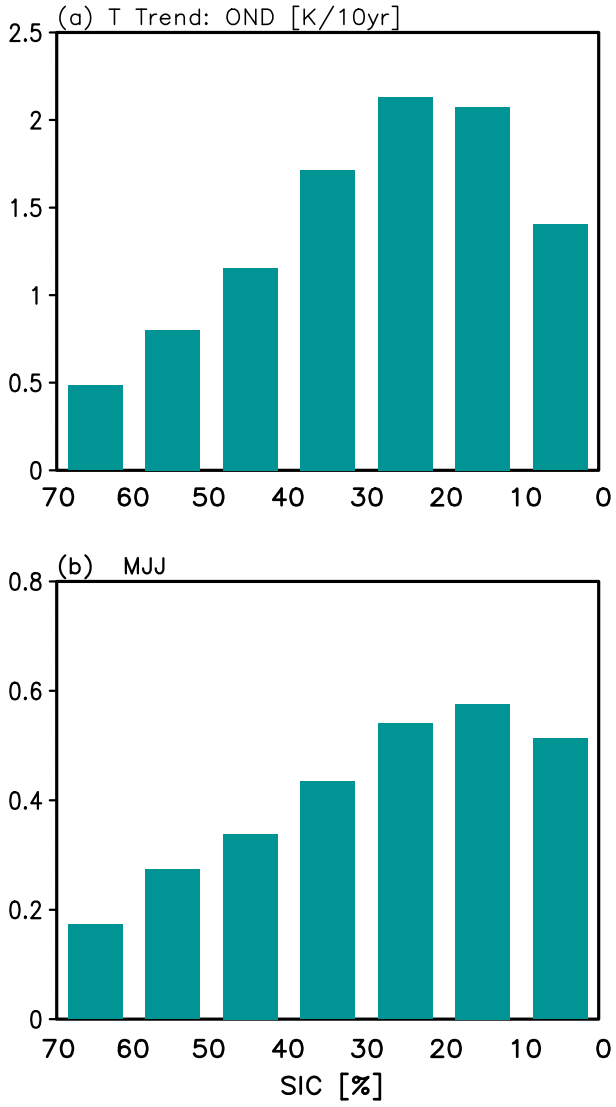

Figure 5. Same as Figure 4a, but Arctic temperature trends in (a) winter (OND) and (b) summer (MJJ). Note that the scales of the *y* axis are different in Figures 5a and 5b.

To illustrate whether this nonlinear sensitivity of AA trend to mean SIC condition is a unique feature of the Arctic Ocean, we compute the relation between the Arctic and global temperature trends and mean SIC in the same way from the five selected models (Figure 4a). It is clearly shown that the dependency of the Arctic temperature trend on the mean SIC is very similar to that of the AA trend (Figures 3b and 4a), indicating that the nonlinear features of the Arctic warming trend are not affected by the model's global sensitivity to a given external forcing but can be explained by the Arctic temperature itself.

On the other hand, it is obvious that the global mean temperature trend is much smaller compared to the Arctic temperature trend as the manifestation of the AA. It is quite distinctive that the global mean temperature trend continuously increases as the mean SIC becomes smaller. The increasing responses of global temperature trends in the five selected models can also be found in the other models that do not have the nonlinear relationship between the AA trend and mean Arctic SIC (not shown). It is important to understand the causes of the increasing warming rates of the global mean temperature in association with the mean SIC or other mean state changes, but this issue is beyond the scope of the present study. This feature is more evident in the temperature trends outside the polar region as marked by the gray bars in Figure 4a.

These differences in the sensitivity of Arctic and global temperature trends to mean SIC imply that the responses of Arctic warming trends may be a unique feature of the Arctic Ocean due to the presence of various feedback processes. One can also find a coherent sensitivity of Arctic warming to sea ice in their temporal variations (Figure 4b). When the reduction in SIC becomes larger (2020s), both Arctic and global temperature trends increase although Arctic temperature trend increases much more than global temperature trend. However, after the slowdown of the rapid reduction in SIC after the 2070s, the Arctic warming trend decreases, whereas the global warming trend is almost constant. These features of Arctic temperature are shown for each five selected models (Figures 4c–4g), although individual models simulate the mean Arctic SIC, its reduction rates, and temperature trends differently during the same time period. This may support our argument that the Arctic temperature is sensitive to the mean SIC in contrast with global temperature.

In order to check whether these nonlinear responses of annual mean Arctic temperature trend to the mean SIC condition vary by season, the Arctic temperature trend in winter (OND) and summer (MJJ) for the mean SIC are examined in the five selected models (Figure 5). The magnitude of the trend is different depending on

season with the large value in winter, consistent with *Deser et al*. [2010] and *Screen and Simmonds* [2010], but overall features of the nonlinear responses to the mean SIC in annual mean Arctic temperature trend (Figure 4a) are still evident in both winter and summer in the five selected models. During sea ice melting season, more solar energy is absorbed in the open ocean, but the near-surface Arctic temperature does not largely increase because the absorbed energy is mainly used to melt the sea ice [*Serreze and Francis*, 2006; *Francis et al*., 2009; *Serreze et al*., 2009; *Deser et al*., 2010; *Screen and Simmonds*, 2010]. Nonetheless, Arctic temperature trend in summer is closely related to the mean SIC as well although its magnitude is much smaller. This indicates that nonlinear responses of Arctic temperature trend to the mean SIC show coherent features in all seasons although the magnitude of the temperature trends and associated processes may be different depending on season.

3.3. Dynamical Understanding of the AA Trends in the Selected Models

In the previous sections, we showed that some models simulate nonlinear relationship between Arctic warming trends and mean SIC. Our analysis from these models suggests that Arctic temperature trend tends to change depending on the sea ice mean state and it may be a coherent feature of Arctic climate. It is possible that these Arctic temperature changes are related to feedback processes associated with the sea ice effect. Thus, we investigate the contribution of the two feedbacks, that is, the surface albedo feedback (SAF) and turbulent heat flux feedback (THF), because the reduction in sea ice is known to amplify Arctic warming through large increases in solar input to the open ocean [*Holland and Bitz*, 2003; *Perovich et al*., 2007] during summer and enhanced sensible and latent (turbulent) heat fluxes from the open ocean [*Serreze and Francis*, 2006; *Serreze et al*., 2009; *Deser et al*., 2010; *Screen and Simmonds*, 2010] during the following winter.

In order to estimate how much of the changes in Arctic warming trend can be reflected by these feedbacks, we examine changes in SAF and THF for the mean SIC condition from the five selected models. The SAF and THF are estimated over the Arctic Ocean [70°–90°N]. Because changes in Arctic temperature may be different for a given external forcing, the SAF and THF for the mean SIC condition are calculated by linearly fitting the changes in net shortwave radiative flux and turbulent heat flux at the surface to a given change in Arctic temperature as follows:

$$\mathrm{SAF\ (or\ THF)} = \frac{\sum \mathrm{HF}'_{\mathrm{SW}}\left(or\ \mathrm{HF}'_{\mathrm{TH}}\right) \times T'}{\sum T'^{2}},$$

where T is near-surface air temperature and $\mathrm{HF_{SW}}$ and $\mathrm{HF_{TH}}$ are net shortwave radiative flux and turbulent (sensible plus latent) heat flux at the surface, respectively. $\mathrm{HF_{SW}}$ and $\mathrm{HF_{TH}}$ are positive for downward and upward, respectively, to illustrate atmospheric temperature warming. Because the ocean surface warmed by downward $\mathrm{HF_{SW}}$ can contribute to decrease the SIC, increased downward $\mathrm{HF_{SW}}$ is considered as a positive feedback. These feedbacks are calculated using monthly mean temperature and heat fluxes data based on the 30 year moving windows and averaged over the corresponding seasons. The prime indicates the deviation from the mean over each 30 year window. Thus, the SAF and THF can provide information of changes in net downward shortwave heat flux and upward turbulent heat flux over the more warmed Arctic temperature changes in response to greenhouse warming. The SAF and THF during winter and summer are shown in Figure 6. For comparison, we also calculate the feedback term based on the annual mean (Figures 6c and 6f).

The winter SAF is almost zero in the all mean SIC conditions (Figure 6a), whereas the summer SAF has a large positive value (Figure 6b), indicating that the SAF acts prominently during the sea ice melting season as noted by *Deser et al*. [2010]. The positive SAF indicates that the surface absorbs more shortwave radiation due to reduced surface albedo associated with the reduction in sea ice, which contributes to Arctic warming through positive feedback. As the mean SIC becomes smaller, the positive SAF increases in response to increasing reduction in sea ice. This feature is found in the annual mean SAF (Figure 6c), but is much distinct in summer SAF because of prominent changes in albedo effect during the sea ice melting season. On the other hand, when the mean SIC reaches a nearly ice-free state (mean SIC of 0–10%, 10–20%), both summer SAF and annual mean SAF decrease somewhat, as shown in the Arctic warming trend (Figure 4a). It may be because the Arctic Ocean is almost free of sea ice and thus changes in surface albedo are no longer as large as before. These changes in SAF can be supported by consistent changes in SIC reduction trend that depends on the mean SIC (Figure 6g).

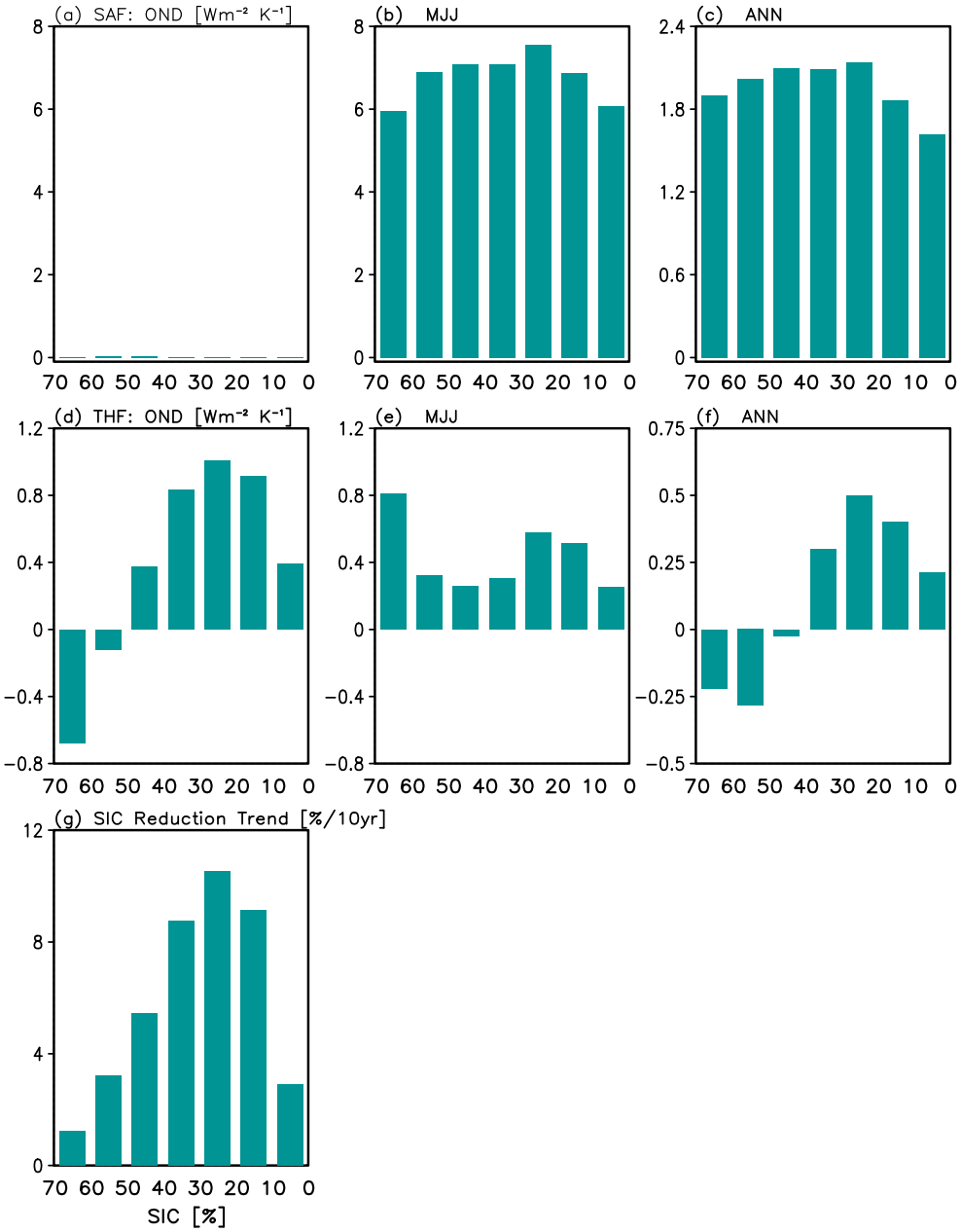

Figure 6. Histograms of (a, d) winter, (b, e) summer, and (c, f) annual mean (ANN) surface albedo feedback (SAF) and turbulent heat flux feedback (THF), and (g) Arctic ASO SIC reduction trends for mean Arctic ASO SIC from the five selected models. The SIC reduction trends are also calculated on moving 30 year windows.

Changes in THF are also highly dependent on varying SIC mean state although the magnitude of summer and annual mean THF is slightly smaller than that of winter THF (Figures 6d–6f). This indicates that the additional heat stored in the ocean during summer due to sea ice reduction is released into the atmosphere prominently during the following winter. It is also interesting that the winter and annual mean THF changes from negative to positive as the mean SIC decreases. This indicates that after the mean SIC becomes smaller than 50% (40%) in winter (annual mean), THF starts to act as part of a positive feedback by the increased reduction in sea ice. This THF change from negative to positive will be discussed in more detail later.

A remarkable feature in Figure 6 is that changes in both SAF and THF for the mean SIC resemble those in Arctic temperature trend, showing a nonlinear relationship with their maxima at the mean SIC of 20–30%.

This indicates that the nonlinear sensitivity of Arctic warming trend to mean SIC condition can be closely related to the changes in SAF and THF, suggesting that the SIC mean state may influence the consequent change in Arctic temperature in association with the shortwave radiation and turbulent heat flux at the surface. Although the SAF and THF show the largest responses in summer and winter, respectively, annual mean SAF and THF are closely related to the mean SIC condition as well. This indicates that seasons when the SAF and THF act prominently are different, but their responses to the mean SIC are consistent with the responses of AA trends. Thus, our result suggests that the sea ice state in summer can be related to the AA trend not only in the season but also in other seasons in association with seasonally varying SAF and THF, depending on the mean SIC. Note that the SAF and THF cannot be also separated, because they are closely interconnected: more downward shortwave radiation due to reduced surface albedo in summer can decrease the sea ice. The sea ice reduction in summer due to strong SAF can contribute to strong THF by providing open-ocean surface in winter, which is critical to determine turbulent heat exchanges between the warm ocean and cold atmosphere. Furthermore, the amplified Arctic temperature sequentially affects sea ice melting during the following summer, leading to enhanced SAF.

So far, we have examined the sensitivity of Arctic warming to mean SIC condition and showed that their nonlinear relationship is closely related to the responses of the SAF and THF, particularly during summer and winter, respectively. The remaining question is why the Arctic warming trends and associated feedback show such nonlinear responses to the mean SIC with their maximums at a critical level of SIC of 20–30%. Also, it is interesting to understand why the THF changes from negative to positive depending on the mean SIC condition. In order to understand associated processes of their changes for each mean SIC condition in detail, we investigate the spatial patterns of mean SIC, SIC trends, and winter THF for the three cases of representative mean SIC conditions including the maximum of Arctic warming trends (i.e., 60–70%, 20–30%, 0–10%) from the five selected models (Figure 7).

In the early stage of global warming (Figure 7a), the large SIC is centered near the pole and the reduction in Arctic sea ice occurs near the ice edge. However, the reduction in sea ice is not spatially uniform in these three cases of mean SIC. For example, in the case of mean SIC of 60–70%, the largest reduction in SIC appears in the Barents Sea. In the case of mean SIC of 20–30% (Figure 7b), the sea ice is significantly reduced over the East Arctic Ocean including the Kara, Barents, and Chukchi Seas, and the large SIC still remains around Greenland and Canada. The reductions are extended toward the Central Arctic which has been covered with very large SIC in the case of a nearly ice-free condition (Figure 7c).

The distribution of corresponding THF exhibits a positive along the reduction region of sea ice and a negative toward the lower latitude of the reduction region in all the three cases of mean SIC (Figures 7d–7f). However, as expected from the spatial patterns of the mean SIC, there are distinctive differences in the THF patterns among the three cases of mean SIC. In the case of mean SIC of 60–70% (Figure 7d), THF is very weak near the pole where SIC is very large and positive THF is found along the reduction region of sea ice that is the edge of the large SIC. The positive THF is associated with the anomalous turbulent heat flux toward the atmosphere due to reduction in sea ice that insulates the relatively warm ocean from the colder atmosphere above. The strong negative THF, mostly located in relatively low latitude, indicates that anomalous turbulent heat flux is toward the ocean in the region where the sea ice is nearly free. It is conceived that the negative THF is because the anomalously warmed atmosphere due to the sea ice reductions or the other heating reduces the air-sea contrast and thus leads to the decreasing heat release to the atmosphere over the ice-free ocean surface. In the early stage of global warming, the negative THF is much stronger than the positive THF over the Arctic Ocean. The positive-negative patterns of THF associated with sea ice are also found in previous studies [*Deser et al*., 2000; *Alexander et al*., 2004; *Magnusdottir et al*., 2004; *Deser et al*., 2010; *Koenigk et al*., 2013; *Peings and Magnusdottir*, 2014].

As the mean SIC becomes smaller, the SIC reduction trend increases so that the positive THF becomes stronger and its area is extended (Figures 7b and 7e). The positive THF is strongest when the mean SIC is at 20–30%, which corresponds to the largest SIC reduction trend (see also Figure 6g). The negative THF is weaker when the mean SIC is at 20–30%. This is probably because anomalous turbulent heat flux toward the ocean in the ice-free region decreases due to the more warmed Arctic atmosphere [e.g., *Koenigk et al*., 2013]. Therefore, the Arctic-averaged THF may be strongest at this SIC mean state.

On the other hand, as the mean SIC is further reduced (0–10%), the SIC reduction appears mainly over the Central Arctic so that the positive THF appears in a more confined region, whereas the negative THF is

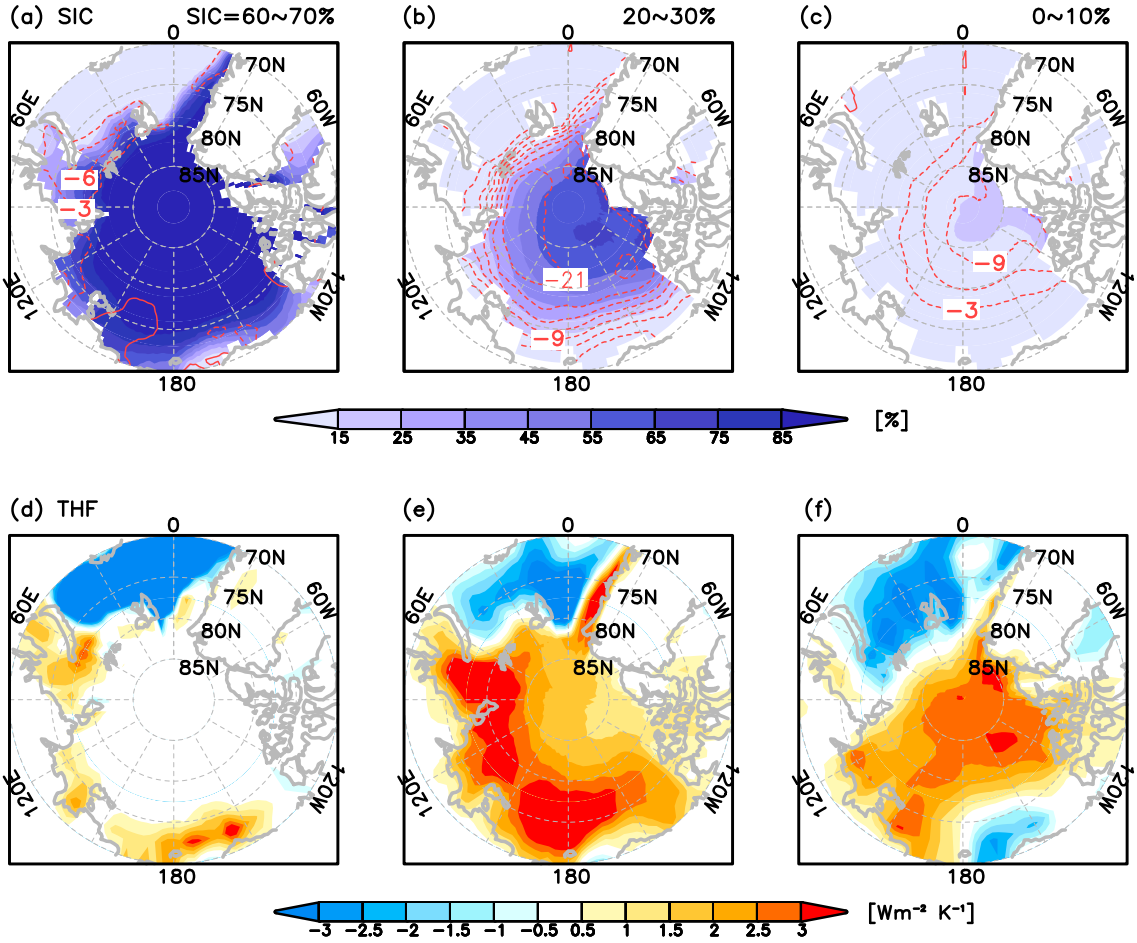

Figure 7. Spatial patterns of (a–c) mean Arctic ASO SIC (shadings) and its trends (red contours, % 10 yr^{-1}) and (d–f) winter THF in the three cases of mean Arctic ASO SIC (60–70%, 20–30%, and 0–10%) from the five selected models. Contour intervals in Figures 7a–7c are 3% 10 yr^{-1}.

extended because of the ice-free open ocean over a larger part of the Arctic Ocean (Figures 7c and 7f). The combination of these distributions of positive and negative THF are reflected to the responses of Arctic-averaged THF to the mean SIC as shown in Figure 6d.

The strongest positive Arctic-averaged THF at the mean SIC of 20–30% can also be explained quantitatively by the combination of positive THF along the reduction regions of sea ice and negative THF over the southern parts of the reduction regions, depending on the mean SIC condition. To show it more clearly, we separate positive and negative THF from whole grids over the Arctic Ocean in Figures 7d–7f. The percentage of corresponding model areas where the positive THF and negative THF, respectively, appear with respect to the total Arctic Ocean, defined as the relative area (=*A*), is also calculated to show the proportions of the positive THF and negative THF over the Arctic Ocean. These values are calculated for each mean SIC, as denoted in Figure 7. Thus, the obtained distributions of positive THF and negative THF as well as *A* for the mean SIC condition can provide information on how the contributions of positive THF and negative THF over the Arctic Ocean change depending on the mean SIC.

Figure 8a shows the changes in magnitude of positive THF and negative THF averaged over the Arctic Ocean for the mean Arctic SIC condition in the five selected models. Together with the results of Figure 7, this result indicates that the positive THF becomes stronger due to the increased reduction in sea ice for the smaller mean SIC as greenhouse warming progresses, whereas changes in negative THF are not as large as those in positive THF for the mean SIC condition.

The value of *A* is also sensitive to the mean SIC condition (Figure 8b). As expected, *A* shows a large increase for positive THF and a decrease for negative THF due to the extension of reduction region of sea ice as the mean

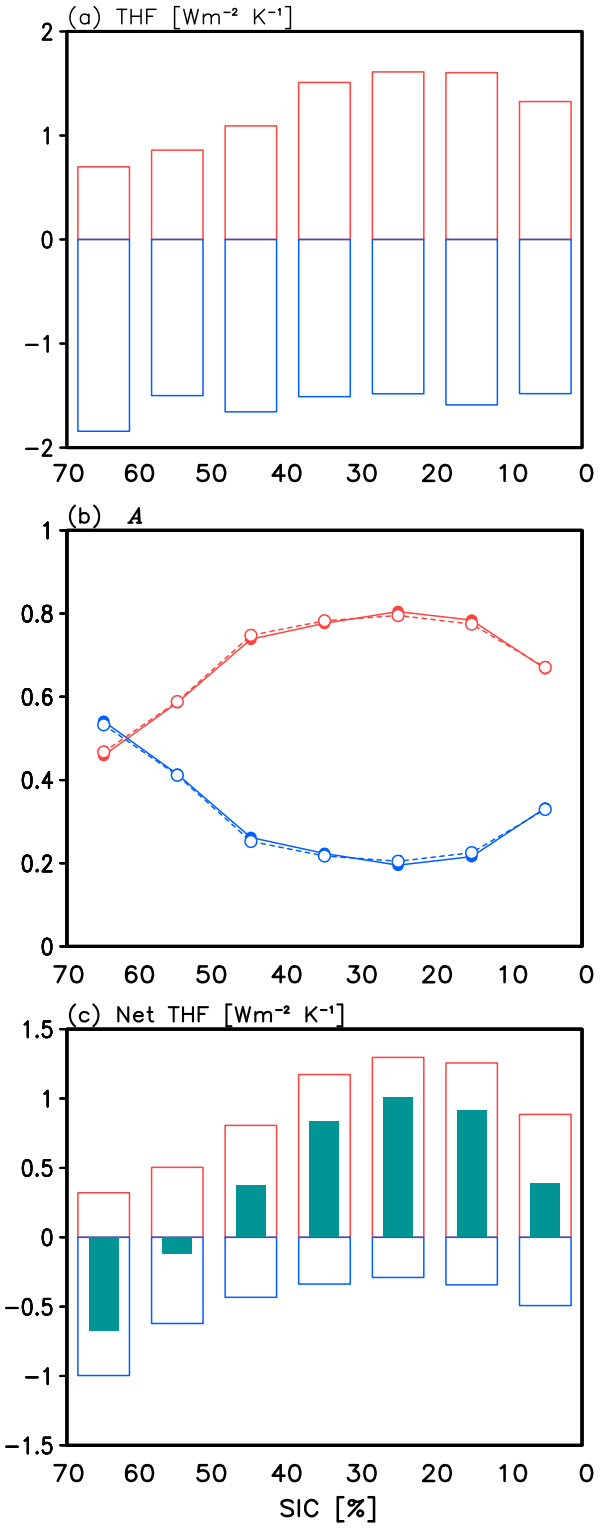

Figure 8. (a) Positive THF (red) and negative THF (blue) averaged over the Arctic Ocean and (b) their relative area (*A*; solid) and (c) net positive THF (red), net negative THF (blue), and total THF (net positive THF + negative THF; dark green) for the seven mean Arctic ASO SIC conditions from the five selected models. The red and blue dashed lines in Figure 8b represent *A* of the regions with and without sea ice reductions for each of the seven mean SIC condition, respectively.

SIC becomes smaller (Figure 7). However, *A* decreases for positive THF and increases for negative THF for a nearly ice-free condition (0–10% and 10–20%), because the sea ice has already been melted and its reduction is confined to the Central Arctic (Figure 7c). These changes in *A* for positive THF and negative THF are in good agreement with those in areas of the region where the sea ice reduces and the ice-free region where the sea ice does not change much, as marked by the dashed lines in Figure 8b, implying that THF is closely related to the local states of sea ice.

Figure 8c confirms the expected tendencies of the net positive THF and negative THF over the Arctic Ocean for the mean Arctic SIC condition in the five selected models. It is evident that the increased net positive THF and decreased net negative THF for smaller mean SIC condition eventually lead to the strongest net contribution of THF as a positive value at the mean SIC of 20–30%, which is the same as the result of Figure 6d. After that, the net THF decreases due to the decrease of net positive THF and to the increase of net negative THF.

4. Summary and Discussion

In this study, we investigated how the sensitivity of Arctic warming changes with respect to the background SIC state under greenhouse warming by analyzing the data sets of the historical and RCP8.5 runs of the CMIP5 during 1960–2100.

Our result reveals that the annual mean AA trend varies depending on the mean SIC condition in the 23 CGCMs, suggesting the importance of sea ice in Arctic temperature change. It is particularly interesting that some models project a variable AA trend in relation to the SIC mean state clearly. In these selected models, the AA trend tends to increase until the mean SIC reaches a critical

level (i.e., 20–30%) and decrease somewhat after that, indicating that Arctic warming does not amplify as much as before as greenhouse warming progresses further. These results can help to understand the state of greatly amplified Arctic warming in the recent decades and provide a potential prediction of the future Arctic climate changes. For example, given that the climatological mean SIC in the observation for 1983–2012 is about 51.1%, our analysis suggests that the recently observed AA [e.g., *Stroeve et al*., 2007; *Screen and Simmonds*, 2010] is in line with the large change of AA trend in the early stage of global warming and its change rate in AA trend will be maintained or accelerated until the mean SIC reaches a certain point.

Comparison between the Arctic and global temperature trends also indicates that the nonlinear responses of Arctic warming trend to mean SIC shown in these models may be a coherent feature of the Arctic Ocean. Further analysis of the associated feedback processes in these models indicates that this nonlinear sensitivity of AA trend to mean SIC condition is closely related to the changes in SAF and THF processes, particularly during summer and winter, respectively, implying that sea ice mean state is closely related to SAF and THF and consequently Arctic warming trend.

It is also noteworthy to discuss why the sensitivity of AA trend to sea ice mean state differs among individual models (Figure 2). In addition to the models showing the nonlinear relationship between them, on which we focused in this paper, several models (CanES2, HadGEM2-AO, HadGEM2-ES, and MIROC5) show the continuously increasing AA trend to mean Arctic SIC (Figures 2t–2w). However, the spatial patterns of SIC and its trend for mean SIC of 0–10% in these models are not largely different from those in the five selected models (not shown). It is shown that if mean SIC of 0–10% is subdivided by smaller intervals, the AA trend for the ice-free condition eventually decreases than before in these models (not shown). The increasing AA trend until very small mean SIC in these models is likely associated with other sea ice conditions, such as its thickness. Further analysis shows that the sea ice for the same mean SIC condition tends to be slightly thicker in these models than in the five selected models and MME over the thickest ice region around Greenland and Canada (not shown). This relatively thick sea ice in these models may support increasing AA trend until the small mean SIC, implying that sea ice thickness can partly influence sea ice melting and consequently AA trend.

We focused on the SIC as a representative of sea ice properties in the present study to illustrate how the Arctic temperature change predicted by the CGCMs under greenhouse warming is related to the characteristics of the sea ice mean state simulated by the CGCMs, but in this sense other properties of sea ice may need to be further considered as well, such as its thickness, transport, and melting/growth. For example, *Holland et al*. [2010] showed that the models with initially thicker ice generally retain more extensive ice throughout the 21st century despite larger increases in net ice melting in the CMIP3 models. *Stroeve et al*. [2012, 2014] also found that several of the CMIP5 models have initially different winter sea ice thickness in the twentieth century, even though their winter sea ice extents are similar to that of the observation.

However, the relationship between the AA trend and mean Arctic sea ice thickness in the present work is not clear in the CMIP5 models, although the AA trend increases with decreasing mean sea ice thickness in some models (not shown). This indicates that the states of SIC rather than sea ice thickness may be more closely related to the AA trend in the CMIP5 models. However, it may be because a considerable diversity in sea ice thickness exists among the models and its patterns are relatively poor compared to the SIC [*Stroeve et al*., 2014]. The sea ice thickness trends in the five selected models also show the nonlinear responses depending on the mean SIC (not shown), indicating that changes in the sea ice thickness in relation to the mean SIC can be associated to the nonlinear responses of AA trend. Thus, this issue should be explored further in future work, which may improve our understanding of Arctic climate changes predicted by CGCMs and the relationship between the Arctic warming and sea ice.

While we mainly focus on the detailed understanding of the relationship between the AA trend and SIC mean state from the obtained results in the five selected models representing the variable AA trend depending to the mean SIC clearly and these results can provide important implications on prediction of the future Arctic climate changes in association with feedback processes between Arctic temperature and sea ice, we may need to discuss how much our understanding from the selected models can be applicable and reliable in the future projections. Although these five models fall within the models simulating the present-day SIC reasonably, it is not likely appropriate to evaluate the reliability of the future projections based on the model's performance in the present-day climate. However, model comparison of SIC and its trends for the mean Arctic SIC shows that at least, under the same mean SIC condition, the spatial patterns of SIC and its trend

in these models are in better agreement with those in the MME of all 23 models (not shown). This implies that our results from the five selected models can be one of the reasonable projections for future Arctic changes regarding the responses of Arctic temperature trend in relation to the evolution of SIC, although other properties of sea ice may in part influence the sea ice melting and thus magnitude of temperature trend in the models.

Although this study only emphasized the roles of sea ice in simulating and predicting changes in the Arctic temperature in the models, it can be expanded by considering together other physical processes, such as clouds, snow cover, and dynamic transport into the Arctic Ocean that may yield nonlinearity in the Arctic temperature changes. Furthermore, these factors can be closely interconnected in association with sea ice. For example, *Hwang et al*. [2011] and *Alexeev and Jackson* [2013] suggested that changes in atmospheric transport are negatively correlated with surface-based AA and surface albedo feedback. Therefore, it would be worthwhile to evaluate comprehensive impacts of these factors on the sensitivity of Arctic warming in a further study.

Acknowledgments

We acknowledge the World Climate Research Programme's Working Group on Coupled Modelling, which is responsible for CMIP, and we thank the climate modeling groups (listed in Table 1 of this paper) for producing and making available their model output. For CMIP the U.S. Department of Energy's Program for Climate Model Diagnosis and Intercomparison provides coordinating support and led development of software infrastructure in partnership with the Global Organization for Earth System Science Portals. The CMIP5 data are available via the Program for Climate Model Diagnosis and Intercomparison (PCMDI) website (http://cmip-pcmdi.llnl.gov/cmip5/). The HadISST data are available at http://www.metoffice.gov.uk/hadobs/hadisst/. JSK is supported by "Polar Academic Project" of the Korea Polar Research Institute (KOPRI), and Korea Meteorological Administration Research and Development Program under grant KMIPA 2015–2091.

References

Alexander, M. A., U. S. Bhatt, J. E. Walsh, M. S. Timlin, J. S. Miller, and J. D. Scott (2004), The atmospheric response to realistic Arctic sea ice anomalies in an AGCM during winter, *J. Clim.*, *17*, 890–905.

Alexeev, V. A., and C. H. Jackson (2013), Polar amplification: Is atmospheric heat transport important?, *Clim. Dyn.*, *41*, 533–547, doi:10.1007/s00382-012-1601-z.

Comiso, J. C., C. L. Parkinson, R. Gersten, and L. Stock (2008), Accelerated decline in the Arctic sea ice cover, *Geophys. Res. Lett.*, *35*, L01703, doi:10.1029/2007GL031972.

Derksen, C., and R. Brown (2012), Spring snow cover extent reductions in the 2008–2012 period exceeding climate model projections, *Geophys. Res. Lett.*, *39*, L19504, doi:10.1029/2012GL053387.

Deser, C., J. E. Walsh, and M. S. Timlin (2000), Arctic sea ice variability in the context of recent atmospheric circulation trends, *J. Clim.*, *13*, 617–633.

Deser, C., R. Tomas, M. Alexander, and D. Lawrence (2010), The seasonal atmospheric response to projected Arctic sea ice loss in the late twenty-first century, *J. Clim.*, *23*, 333–351.

Devasthale, A., J. Sedlar, T. Koenigk, and E. J. Fetzer (2013), The thermodynamic state of the Arctic atmosphere observed by AIRS: Comparisons during the record minimum sea ice extents of 2007 and 2012, *Atmos. Chem. Phys.*, *13*, 7441–7450, doi:10.5194/acp-13-7441-2013.

Eisenman, I., N. Untersteiner, and J. S. Wettlaufer (2007), On the reliability of simulated Arctic sea ice in global climate models, *Geophys. Res. Lett.*, *34*, L10501, doi:10.1029/2007GL029914.

Francis, J. A., W. Chan, D. J. Leathers, J. R. Miller, and D. E. Veron (2009), Winter Northern Hemisphere weather patterns remember summer Arctic sea ice extent, *Geophys. Res. Lett.*, *36*, L07503, doi:10.1029/2009GL037274.

Graversen, R. G., and M. Wang (2009), Polar amplification in a coupled climate model with locked albedo, *Clim. Dyn.*, *33*, 629–643, doi:10.1007/s00382-009-0535-6.

Graversen, R. G., T. Mauritsen, M. Tjernstrom, E. Kallen, and G. Svensson (2008), Vertical structure of recent Arctic warming, *Nature*, *451*(7174), 53–56, doi:10.1038/nature06502.

Holland, M. M., and C. M. Bitz (2003), Polar amplification of climate change in coupled models, *Clim. Dyn.*, *21*, 221–232.

Holland, M. M., C. M. Bitz, L. B. Tremblay, and D. A. Bailey (2008), The role of natural versus forced change in future rapid summer Arctic ice loss, in *Arctic Sea Ice Decline: Observations, Projections, Mechanisms, and Implications*, *Geophys. Monogr*, vol. 180, edited by E. T. DeWeaver, C. M. Bitz, and L.-B. Tremblay, pp. 133–150, AGU, Washington, D. C.

Holland, M. M., M. C. Serreze, and J. Stroeve (2010), The sea ice mass budget of the Arctic and its future change as simulated by coupled climate models, *Clim. Dyn.*, *34*, 185–200, doi:10.1007/s00382-008-0493-4.

Honda, M., J. Inoue, and S. Yamane (2009), Influence of low Arctic sea-ice minima on anomalously cold Eurasian winters, *Geophys. Res. Lett.*, *36*, L08707, doi:10.1029/2008GL037079.

Hwang, Y.-. T., D. M. W. Frierson, and J. E. Kay (2011), Coupling between Arctic feedbacks and changes in poleward energy transport, *Geophys. Res. Lett.*, *38*, L17704, doi:10.1029/2011GL048546.

Jeong, J.-H., J.-S. Kug, B.-M. Kim, S.-K. Min, H. W. Linderholm, C.-H. Ho, D. Rayner, D. Chen, and S.-Y. Jun (2012), Greening in the circumpolar high-latitude may amplify warming in the growing season, *Clim. Dyn.*, *38*, 1421–1431, doi:10.1007/s00382-011-1142-x.

Jeong, J.-H., J.-S. Kug, H. W. Linderholm, D. Chen, B.-M. Kim, and S.-Y. Jun (2014), Intensified Arctic warming under greenhouse warming by vegetation-atmosphere-sea ice interaction, *Environ. Res. Lett.*, *9*, 094007, doi:10.1088/1748-9326/9/9/094007.

Kattsov, V., V. Ryabinin, J. Overland, M. Serreze, M. Visbeck, J. Walsh, W. Meier, and X. Zhang (2010), Arctic sea ice change: A grand challenge of climate science, *J. Glaciol.*, *56*(200), 1115–1121, doi:10.3189/002214311796406176.

Kay, J. E., M. M. Holland, and A. Jahn (2011), Inter-annual to multi-decadal Arctic sea ice extent trends in a warming world, *Geophys. Res. Lett.*, *38*, L15708, doi:10.1029/2011GL048008.

Koenigk, T., and L. Brodeau (2014), Ocean heat transport into the Arctic in the twentieth and twenty-first century in EC-Earth, *Clim. Dyn.*, *42*, 3101–3120, doi:10.1007/s00382-013-1821-x.

Koenigk, T., L. Brodeau, R. G. Graversen, J. Karlsson, G. Svensson, M. Tjernström, U. Willen, and K. Wyser (2013), Arctic climate change in 21st century CMIP5 simulations with EC-Earth, *Clim. Dyn.*, *40*, 2720–2742, doi:10.1007/s00382-012-1505-y.

Kug, J.-S., D.-H. Choi, F.-F. Jin, W.-T. Kwon, and H.-L. Ren (2010), Role of synoptic eddy feedback on polar climate responses to the anthropogenic forcing, *Geophys. Res. Lett.*, *37*, L14704, doi:10.1029/2010GL043673.

Kug, J.-S., J.-H. Jeong, Y.-S. Jang, B.-M. Kim, C. Folland, S.-K. Min, and S.-W. Son (2015), Two distinct influences of Arctic warming on cold winters over North America and East Asia, *Nat. Geosci.*, *8*, 759–762, doi:10.1038/NGEO2517.

Kwok, R. (2011), Observational assessment of Arctic Ocean sea ice motion, export, and thickness in CMIP3 climate simulations, *J. Geophys. Res.*, *116*, C00D05, doi:10.1029/2011JC007004.

Liu J., Song M., Horton R. M., Hu Y. (2013), Reducing spread in climate model projections of a September ice-free Arctic, *Proc. Natl. Acad. Sci. U.S.A.*, *110*(31), 12,571–12,576. [Available at www.pnas.org/cgi/doi/10.1073/pnas.1219716110.]
Liu, Y., J. R. Key, and X. Wang (2008), The influence of changes in cloud cover on recent surface temperature trends in the Arctic, *J. Clim.*, *21*, 705–715.
Magnusdottir, G., C. Deser, and R. Saravanan (2004), The effects of North Atlantic SST and sea ice anomalies on the winter circulation in CCM3. Part I: Main features and storm-track characteristics of the response, *J. Clim.*, *17*, 857–876.
Mahlstein, I., and R. Knutti (2012), September Arctic sea ice predicted to disappear near 2°C global warming above present, *J. Geophys. Res.*, *117*, D06104, doi:10.1029/2011JD016709.
Maslowski, W., J. C. Kinney, M. Higgins, and A. Roberts (2012), The future of Arctic sea ice, *Annu. Rev. Earth Planet. Sci.*, *40*, 625–654.
Massonnet, F., T. Fichefet, H. Goosse, C. M. Bitz, G. Philippon-Berthier, M. M. Holland, and P.-Y. Barriat (2012), Constraining projections of summer Arctic sea ice, *Cryosphere*, *6*, 1383–1394, doi:10.5194/tc-6-1383-2012.
Overland, J. E., and M. Wang (2010), Large-scale atmospheric circulation changes are associated with the recent loss of Arctic sea ice, *Tellus*, *62A*, 1–9.
Overland, J. E., K. Wood, and M. Wang (2011), Warm Arctic–cold continents: Climate impacts of the newly open Arctic Sea, *Polar Res.*, *30*, 15,787, doi:10.3402/polar.v30i0.15787.
Parkinson, C. L., and J. C. Comiso (2013), On the 2012 record low Arctic sea ice cover: Combined impact of preconditioning and an August storm, *Geophys. Res. Lett.*, *40*, 1356–1361, doi:10.1002/grl.50349.
Peings, Y., and G. Magnusdottir (2014), Response of the wintertime Northern Hemisphere atmospheric circulation to current and projected Arctic sea ice decline: A numerical study with CAM5, *J. Clim.*, *27*, 244–264.
Perlwitz, J., M. Hoerling, and R. Dole (2015), Arctic tropospheric warming: Causes and linkages to lower latitudes, *J. Clim.*, *28*, 2154–2167, doi:10.1175/JCLI-D-14-00095.1.
Perovich, D. K., B. Light, H. Eicken, K. F. Jones, K. Runciman, and S. V. Nghiem (2007), Increasing solar heating of the Arctic Ocean and adjacent seas, 1979–2005: Attribution and role in the ice-albedo feedback, *Geophys. Res. Lett.*, *34*, L19505, doi:10.1029/2007GL031480.
Pithan, F., and T. Mauritsen (2014), Arctic amplification dominated by temperature feedbacks in contemporary climate models, *Nat. Geosci.*, *7*, 181–184, doi:10.1038/ngeo2071.
Polyakov I. V., G. V. Alekseev, R. V. Bekryaev, U. Bhatt, R. L. Colony, M. A. Johnson, V. P. Karklin, A. P. Makshtas, D. Walsh, A. V. Yulin (2002), Observationally based assessment of polar amplification of global warming, *Geophys. Res. Lett.*, *29*(18), 1878, doi:10.1029/2001GL011111
Rayner N. A., D. E. Parker, E. B. Horton, C. K. Folland, L. V. Alexander, D. P. Rowell, E. C. Kent, A. Kaplan (2003), Global analyses of sea surface temperature, sea ice, and night marine air temperature since the late nineteenth century, *J. Geophys. Res.*, *108*(D14), 4407, doi:10.1029/2002JD002670
Rudeva, I., and I. Simmonds (2015), Variability and trends of global atmospheric frontal activity and links with large-scale modes of variability, *J. Clim.*, *28*, 3311–3330, doi:10.1175/JCLI-D-14-00458.1.
Screen, J. A., and I. Simmonds (2010), Increasing fall-winter energy loss from the Arctic Ocean and its role in Arctic temperature amplification, *Geophys. Res. Lett.*, *37*, L16707, doi:10.1029/12010GL044136.
Screen, J. A., and I. Simmonds (2013), Exploring links between Arctic amplification and mid-latitude weather, *Geophys. Res. Lett.*, *40*, 959–964, doi:10.1002/grl.50174.
Screen, J. A., I. Simmonds, and K. Keay (2011), Dramatic interannual changes of perennial Arctic sea ice linked to abnormal summer storm activity, *J. Geophys. Res.*, *116*, D15105, doi:10.1029/2011JD015847.
Screen, J. A., C. Deser, and I. Simmonds (2012), Local and remote controls on observed Arctic warming, *Geophys. Res. Lett.*, *39*, L10709, doi:10.1029/2012GL051598.
Screen, J. A., C. Deser, I. Simmonds, and R. Tomas (2014), Atmospheric impacts of Arctic sea-ice loss, 1979–2009: Separating forced change from atmospheric internal variability, *Clim. Dyn.*, *43*, 333–344, doi:10.1007/s00382-013-1830-9.
Serreze, M., and J. Francis (2006), The Arctic amplification debate, *Clim. Change*, *76*, 241–264.
Serreze, M., A. Barrett, J. Stroeve, D. Kindig, and M. Holland (2009), The emergence of surface-based Arctic amplification, *Cryosphere*, *3*, 11–19.
Simmonds, I. (2015), Comparing and contrasting the behaviour of Arctic and Antarctic sea ice over the 35 year period 1979–2013, *Ann. Glaciol.*, *56*(69), 18–28, doi:10.3189/2015AoG69A909.
Simmonds, I., and P. D. Govekar (2014), What are the physical links between Arctic sea ice loss and Eurasian winter climate?, *Environ. Res. Lett.*, *9*, 101003, doi:10.1088/1748-9326/9/10/101003.
Stroeve, J. C., V. Kattsov, A. Barrett, M. Serreze, T. Pavlova, M. Holland, and W. N. Meier (2012), Trends in Arctic sea ice extent from CMIP5, CMIP3 and observations, *Geophys. Res. Lett.*, *39*, L16502, doi:10.1029/2012GL052676.
Stroeve, J., M. M. Holland, W. Meier, T. Scambos, and M. Serreze (2007), Arctic sea ice decline: Faster than forecast, *Geophys. Res. Lett.*, *34*, L09501, doi:10.1029/2007GL029703.
Stroeve, J., M. Serreze, S. Drobot, S. Gearheard, M. Holland, J. Maslanik, W. Meier, and T. Scambos (2008), Arctic sea ice extent plummets in 2007, *Eos Trans. AGU*, *89*(2), doi:10.1029/2008EO020001.
Stroeve, J., A. Barrett, M. Serreze, and A. Schweiger (2014), Using records from submarine, aircraft and satellites to evaluate climate model simulations of Arctic sea ice thickness, *Cryosphere*, *8*, 1839–1854, doi:10.5194/tc-8-1839-2014.
Symon, C., L. Arris, and B. Heal (2004), *Arctic Climate Impact Assessment*, Cambridge Univ Press, New York.
Taylor, K. E., R. J. Stouffer, and G. A. Meehl (2012), An overview of CMIP5 and the experiment design, *Bull. Am. Meteorol. Soc.*, *93*(4), 485–498, doi:10.1175/BAMS-D-11-00094.1.
Wang, M., and J. E. Overland (2009), A sea ice free summer Arctic within 30 years?, *Geophys. Res. Lett.*, *36*, L07502, doi:10.1029/2009GL037820.
Wang, M., and J. E. Overland (2012), A sea ice free summer Arctic within 30 years: An update from CMIP5 models, *Geophys. Res. Lett.*, *39*, L18501, doi:10.1029/2012GL052868.
Xu, J., A. M. Powell Jr., and L. Zhao (2013), Intercomparison of temperature trends in IPCC CMIP5 simulations with observations, reanalyses and CMIP3 models, *Geosci. Model. Dev.*, *6*, 1705–1714, doi:10.5194/gmd-6-1705-2013.
Yim, B. Y., H. S. Min, and J.-S. Kug (2016), Inter-model diversity in jet stream changes and its relation to Arctic climate in CMIP5, *Clim. Dyn.*, doi:10.1007/s00382-015-2833-5.
Zhang, X., and J. E. Walsh (2006), Toward a seasonally ice-covered Arctic Ocean: Scenarios from the IPCC AR4 model simulations, *J. Clim.*, *19*, 1730–1747.